

NATIONAL UNIVERSITY OF HO CHI MINH CITY  
UNIVERSITY OF SCIENCE

UNDERGRADUATE THESIS

Three-band tight binding model for TMD monolayers  
in the presence of a magnetic field

Ho Chi Minh City, 2025

---

Student: Tran Khoi Nguyen

Supervisor: Dr. Huynh Thanh Duc

# TABLE OF CONTENTS

<b>TABLE OF CONTENTS</b>	<b>1</b>
<b>LIST OF FIGURES</b>	<b>2</b>
<b>1 INTRODUCTION</b>	<b>3</b>
<b>2 METHOD</b>	<b>4</b>
2.1 Three-band tight binding method without magnetic field . . . . .	4
2.2 Three-band tight binding method under a magnetic field . . . . .	4
2.3 Spin-orbit coupling . . . . .	9
2.4 Landau levels . . . . .	11
<b>3 DISCUSSION AND FUTURE WORK</b>	<b>13</b>
<b>REFERENCES</b>	<b>14</b>
<b>A Construct matrix</b>	<b>16</b>
<b>B Harper's equation</b>	<b>17</b>
<b>C Phase factor</b>	<b>20</b>

## LIST OF FIGURES

2.1	Top view of monolayer $MX_2$ . The large sphere is $M$ atom and the small sphere is $X$ . . . . .	5
2.2	Site index . . . . .	7
2.3	Hofstadter's butterfly for one band $ dz\rangle \equiv  \phi_1^1(x, y)\rangle$ (left) and all band(right) with $q = 797$ and vary $p$ from 1 to $q$ with field strength $B_0 = 4.6928 \times 10^4$ T. . . . .	10
2.4	(a) Same plot as Fig 2.3 but we consider a small area and (b) is the Landau fan diagram show for the first $n = 10$ levels near the bottom of the conduction band for a magnetic field up to $B = 100 T$ . . . . .	12

# CHAPTER 1

## INTRODUCTION

## CHAPTER 2

### METHOD

#### 2.1 Three-band tight binding method without magnetic field

The time-independent Schrödinger equation for an electron in the crystal has the form

$$\left[ -\frac{\hbar^2 \nabla^2}{2m} + U_0(\mathbf{r}) \right] \quad (2.1)$$

#### 2.2 Three-band tight binding method under a magnetic field

Under a uniform magnetic field given by a vector potential  $\mathbf{A}(\mathbf{r})$  the single electron Hamiltonian changes into

$$H = \frac{(-i\hbar \nabla + e\mathbf{A}(\mathbf{r}))^2}{2m} + U_0(\mathbf{r}) + g^* \mu_B \mathbf{B} \cdot \mathbf{L}, \quad (2.2)$$

where  $\mu_B = \frac{e\hbar}{2m}$  is Bohr magneton,  $g^*$  is an effective Landé g-factor,  $\mathbf{B} = \nabla \times \mathbf{A}$  is the uniform magnetic field, and  $\mathbf{L}$  is the angular momentum. It is possible to add a phase

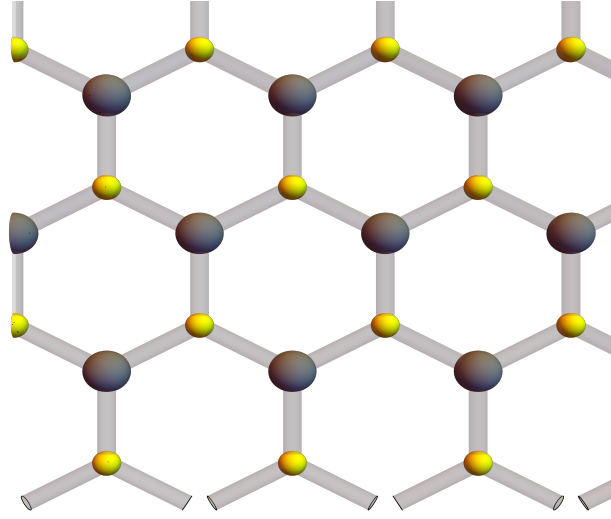


Figure 2.1: Top view of monolayer  $MX_2$ . The large sphere is  $M$  atom and the small sphere is  $X$ .

factor to the tight binding wavefunction

$$\psi_{\lambda,\mathbf{k}}(\mathbf{r}) = \sum_{j=1}^3 C_j^\lambda \sum_{\mathbf{R}} e^{i\mathbf{k}\cdot\mathbf{R}} e^{i\theta_{\mathbf{R}}(\mathbf{r})} \phi_j(\mathbf{r} - \mathbf{R}). \quad (2.3)$$

We now have

$$H_{jj'}(\mathbf{k}) = H'_{jj'}(\mathbf{k}) + H^Z_{jj'}(\mathbf{k}), \quad (2.4)$$

where

$$\begin{aligned} H_{jj'}(\mathbf{k}) &= \sum_{\mathbf{R}} e^{i\mathbf{k}\cdot\mathbf{R}} \langle \phi_j(\mathbf{r}) | e^{-i\theta_0(\mathbf{r})} \left[ \frac{(-i\hbar\nabla + e\mathbf{A}(\mathbf{r}))^2}{2m} + U_0(\mathbf{r}) \right] e^{i\theta_{\mathbf{R}}(\mathbf{r})} | \phi_{j'}(\mathbf{r} - \mathbf{R}) \rangle \\ &= \sum_{\mathbf{R}} e^{i\mathbf{k}\cdot\mathbf{R}} \langle \phi_j(\mathbf{r}) | e^{i(\theta_{\mathbf{R}} - \theta_0)} \left[ \frac{(-i\hbar\nabla + e\mathbf{A} + \hbar\nabla\theta_{\mathbf{R}})^2}{2m} + U_0(\mathbf{r}) \right] | \phi_{j'}(\mathbf{r} - \mathbf{R}) \rangle, \end{aligned} \quad (2.5)$$

and

$$H_{jj'}^Z(\mathbf{k}) = g^* \mu_B \mathbf{B} \cdot \sum_{\mathbf{R}} \langle \phi_j(\mathbf{r}) | e^{i(\theta_{\mathbf{R}} - \theta_0)} \mathbf{L} | \phi_{j'}(\mathbf{r} - \mathbf{R}) \rangle. \quad (2.6)$$

By choosing  $\theta_{\mathbf{R}} = -\frac{e}{\hbar} \int_{\mathbf{R}}^{\mathbf{r}} \mathbf{A}(\mathbf{r}') \cdot d\mathbf{r}'$  as Peierls substitution, the Hamiltonian in Eq. (4) now reads

$$\begin{aligned} H_{jj'}(\mathbf{k}) &= \sum_{\mathbf{R}} e^{i\mathbf{k} \cdot \mathbf{R}} \langle \phi_j(\mathbf{r}) | e^{-\frac{ie}{\hbar} \int_{\mathbf{R}}^{\mathbf{r}} \mathbf{A}(\mathbf{r}') \cdot d\mathbf{r}' + \frac{ie}{\hbar} \int_0^{\mathbf{r}} \mathbf{A}(\mathbf{r}') \cdot d\mathbf{r}'} \left[ -\frac{\hbar^2 \nabla^2}{2m} + U_0(\mathbf{r}) \right] | \phi_{j'}(\mathbf{r} - \mathbf{R}) \rangle \\ &= \sum_{\mathbf{R}} e^{i\mathbf{k} \cdot \mathbf{R}} e^{\frac{ie}{\hbar} \int_0^{\mathbf{R}} \mathbf{A}(\mathbf{r}') \cdot d\mathbf{r}'} \langle \phi_j(\mathbf{r}) | e^{-\frac{ie}{\hbar} \Phi_{\mathbf{R},\mathbf{r},0}} \left[ -\frac{\hbar^2 \nabla^2}{2m} + U_0(\mathbf{r}) \right] | \phi_{j'}(\mathbf{r} - \mathbf{R}) \rangle, \end{aligned} \quad (2.7)$$

where  $\Phi_{\mathbf{R},\mathbf{r},0} = \oint_{\mathbf{R},\mathbf{r},0} \mathbf{A}(\mathbf{r}') \cdot d\mathbf{r}'$  is the closed loop line integral of  $\mathbf{A}$  along the triangle points  $\mathbf{R}, \mathbf{r}, 0$ , and  $\int_0^{\mathbf{R}} \mathbf{A}(\mathbf{r}') \cdot d\mathbf{r}'$  is the path integral along the two points  $\mathbf{R}, 0$ . Besides that, we have used the fact that

$$\int_{\mathbf{R}}^{\mathbf{r}} \mathbf{A}(\mathbf{r}') \cdot d\mathbf{r}' + \int_{\mathbf{r}}^0 \mathbf{A}(\mathbf{r}') \cdot d\mathbf{r}' = \Phi_{\mathbf{R},\mathbf{r},0} - \int_0^{\mathbf{R}} \mathbf{A}(\mathbf{r}') \cdot d\mathbf{r}'. \quad (2.8)$$

We can show that the flux term  $\Phi_{\mathbf{R},\mathbf{r},0}$  is negligibly small<sup>1</sup> by two observations. When  $\mathbf{r}$  is far away from the lattice points  $\mathbf{R}$  and  $0$ , the flux is large but since the atomic orbitals are highly localized at these two lattice points, the value of the hopping term is very small and the whole hopping term goes to zero. While  $\mathbf{r}$  is at or near any of these lattice points, the triangle formed is small, and assuming small magnetic field, the flux term  $\Phi_{\mathbf{R},\mathbf{r},0}$  goes to zero, which giving us the Hamiltonian as

$$H_{jj'}(\mathbf{k}) = \sum_{\mathbf{R}} e^{i\mathbf{k} \cdot \mathbf{R}} e^{\frac{ie}{\hbar} \int_0^{\mathbf{R}} \mathbf{A}(\mathbf{r}') \cdot d\mathbf{r}'} \langle \phi_j(\mathbf{r}) | \left[ -\frac{\hbar^2 \nabla^2}{2m} + U_0(\mathbf{r}) \right] | \phi_{j'}(\mathbf{r} - \mathbf{R}) \rangle, \quad (2.9)$$

$$H_{jj'}^Z(\mathbf{k}) = g^* \mu_B \mathbf{B} \cdot \sum_{\mathbf{R}} e^{i\mathbf{k} \cdot \mathbf{R}} e^{\frac{ie}{\hbar} \int_0^{\mathbf{R}} \mathbf{A}(\mathbf{r}') \cdot d\mathbf{r}'} \langle \phi_j(\mathbf{r}) | \mathbf{L} | \phi_{j'}(\mathbf{r} - \mathbf{R}) \rangle. \quad (2.10)$$

Considering only nearest neighbor(NN) hopping, Eq (2.9) becomes

$$\begin{aligned}
H_{\mu\mu'}^{jj'}(\mathbf{k}) &= \sum_{\mathbf{R}} e^{\frac{ie}{\hbar} \int_0^{\mathbf{R}} \mathbf{A}(\mathbf{r}') \cdot d\mathbf{r}'} e^{i\mathbf{k} \cdot \mathbf{R}} E_{\mu\mu'}^{jj'}(\mathbf{R}) \\
&= E_{\mu\mu'}^{jj'}(\mathbf{0}) + e^{\frac{ie}{\hbar} \int_0^{\mathbf{R}_1} \mathbf{A}(\mathbf{r}') \cdot d\mathbf{r}'} e^{i\mathbf{k} \cdot \mathbf{R}_1} E_{\mu\mu'}^{jj'}(\mathbf{R}_1) \\
&+ e^{\frac{ie}{\hbar} \int_0^{\mathbf{R}_2} \mathbf{A}(\mathbf{r}') \cdot d\mathbf{r}'} e^{i\mathbf{k} \cdot \mathbf{R}_2} E_{\mu\mu'}^{jj'}(\mathbf{R}_2) + e^{\frac{ie}{\hbar} \int_0^{\mathbf{R}_3} \mathbf{A}(\mathbf{r}') \cdot d\mathbf{r}'} e^{i\mathbf{k} \cdot \mathbf{R}_3} E_{\mu\mu'}^{jj'}(\mathbf{R}_3) \\
&+ e^{\frac{ie}{\hbar} \int_0^{\mathbf{R}_4} \mathbf{A}(\mathbf{r}') \cdot d\mathbf{r}'} e^{i\mathbf{k} \cdot \mathbf{R}_4} E_{\mu\mu'}^{jj'}(\mathbf{R}_4) + e^{\frac{ie}{\hbar} \int_0^{\mathbf{R}_5} \mathbf{A}(\mathbf{r}') \cdot d\mathbf{r}'} e^{i\mathbf{k} \cdot \mathbf{R}_5} E_{\mu\mu'}^{jj'}(\mathbf{R}_5) \\
&+ e^{\frac{ie}{\hbar} \int_0^{\mathbf{R}_6} \mathbf{A}(\mathbf{r}') \cdot d\mathbf{r}'} e^{i\mathbf{k} \cdot \mathbf{R}_6} E_{\mu\mu'}^{jj'}(\mathbf{R}_6).
\end{aligned} \tag{2.11}$$

In the presence of a perpendicular magnetic field  $\mathbf{B}\hat{z}$  with the vector potential  $\vec{A} = (0, Bx, 0)$ . For convenience, let us switch to a shorthand notation for these extra terms and define

$$\theta_{m,n}^{m',n'} \equiv -\frac{e}{\hbar} \int_{m,n}^{m',n'} \vec{A} \cdot d\mathbf{r}. \tag{2.12}$$

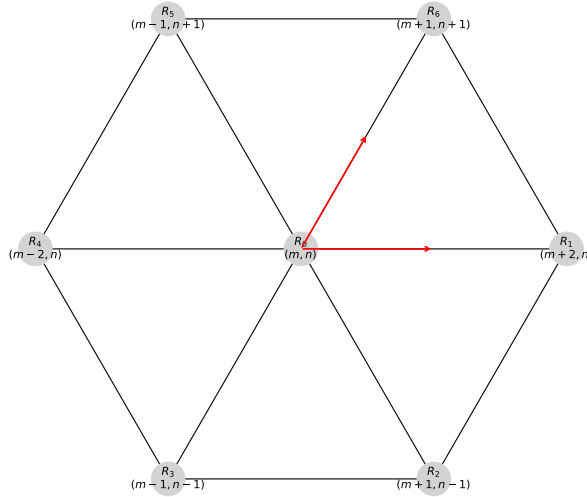


Figure 2.2: Site index

With the given Landau gauge, the line intergral  $\int \vec{A} \cdot d\mathbf{r}$  is evaluated to  $\int Bx dy$ . Let us now express the Hamiltonian from the zero-field are given by<sup>2</sup> with the transform



hopping parameters, noting that the NN coordinates are  $x = \frac{ma}{2}$  ( $m = \pm 1, \pm 2$ ) and  $y = \frac{na\sqrt{3}}{2}$  ( $n = 0, \pm 1$ ),  $a$  being the lattice constant, are shown in Fig (2.2). Since  $dy = 0$  along the  $x$  direction,  $\theta_{m,n}^{m\pm 2,n} = 0$ , and using *ansatz*  $x = \frac{ma}{2}$  for lattice site, the  $\theta_{m,n}^{m',n'}$  can be written as

$$\theta_{m,n}^{m',n'} = \begin{cases} 0 & m' = m \pm 2, n' = n \\ \pm \frac{e}{\hbar} \frac{Ba^2\sqrt{3}}{2} (m + 1/2) & m' = m + 1, n' = n \pm 1 \\ \pm \frac{e}{\hbar} \frac{Ba^2\sqrt{3}}{2} (m - 1/2) & m' = m - 1, n' = n \pm 1 \end{cases} \quad (2.13)$$

Identifying  $\frac{Ba^2\sqrt{3}}{2}$  as the magnetic flux  $\Phi$  passing through per unit cell and  $\hbar/e$  as the flux quantum  $\Phi_0$ , then we have

$$\begin{aligned} H_{\mu\mu'}^{jj'}(\mathbf{k}) &= E_{\mu\mu'}^{jj'}(\mathbf{0}) + e^{i\theta_{m,n}^{m',n'}} e^{i\mathbf{k}\cdot\mathbf{R}_1} E_{\mu\mu'}^{jj'}(\mathbf{R}_1) + e^{i\theta_{m,n}^{m',n'}} e^{i\mathbf{k}\cdot\mathbf{R}_2} E_{\mu\mu'}^{jj'}(\mathbf{R}_2) \\ &+ e^{i\theta_{m,n}^{m',n'}} e^{i\mathbf{k}\cdot\mathbf{R}_3} E_{\mu\mu'}^{jj'}(\mathbf{R}_3) + e^{i\theta_{m,n}^{m',n'}} e^{i\mathbf{k}\cdot\mathbf{R}_4} E_{\mu\mu'}^{jj'}(\mathbf{R}_4) \\ &+ e^{i\theta_{m,n}^{m',n'}} e^{i\mathbf{k}\cdot\mathbf{R}_5} E_{\mu\mu'}^{jj'}(\mathbf{R}_5) + e^{i\theta_{m,n}^{m',n'}} e^{i\mathbf{k}\cdot\mathbf{R}_6} E_{\mu\mu'}^{jj'}(\mathbf{R}_6). \end{aligned} \quad (2.14)$$

The Hamiltonian depends on the site index  $m$  and does not invariant under the translation of a lattice vector along the  $x$  axis. In order to restore this invariance, we can look at the case where the ratio of magnetic flux and flux quanta is a rational number  $\Phi/\Phi_0 = p/q$ . This mean, we have expand the unit cell in the  $x$  direction, the Hamiltonian becomes invariant under translational, allowing us to define what we will call the magnetic unit cell, which is consisting of  $q$   $M$ -atoms. We define a new basis set of  $3q$  atomic orbitals  $\phi_\mu^j(x, y) = \phi_\mu^j(ma/2, y)$  where  $m = 1, 2, \dots, q$ . Note that

$$\begin{cases} e^{ik_x a} \phi_\mu^j(m\frac{a}{2}, y) = \phi_\mu^j((m+2)\frac{a}{2}, y) & ; e^{-ik_x a} \phi_\mu^j(m\frac{a}{2}, y) = \phi_\mu^j((m-2)\frac{a}{2}, y) \\ e^{ik_x \frac{a}{2}} \phi_\mu^j(m\frac{a}{2}, y) = \phi_\mu^j((m+1)\frac{a}{2}, y) & ; e^{-ik_x \frac{a}{2}} \phi_\mu^j(m\frac{a}{2}, y) = \phi_\mu^j((m-1)\frac{a}{2}, y) \end{cases} \quad (2.15)$$

Consequently the Hamiltonian matrix in the new basis is written as

$$\begin{aligned}
H_{\mu\mu'}^{jj'}(\mathbf{k}) = & E_{\mu\mu'}^{jj'}(\mathbf{0}) + e^{i\theta_{m,n}^{m',n'}} E_{\mu\mu'}^{jj'}(\mathbf{R}_1) \delta_{m,m+2} \delta_{n,n} + e^{i\theta_{m,n}^{m',n'}} E_{\mu\mu'}^{jj'}(\mathbf{R}_2) \delta_{m,m+1} \delta_{n,n-1} \\
& + e^{i\theta_{m,n}^{m',n'}} E_{\mu\mu'}^{jj'}(\mathbf{R}_3) \delta_{m,m-1} \delta_{n,n-1} + e^{i\theta_{m,n}^{m',n'}} E_{\mu\mu'}^{jj'}(\mathbf{R}_4) \delta_{m,m+2} \delta_{n,n} \\
& + e^{i\theta_{m,n}^{m',n'}} E_{\mu\mu'}^{jj'}(\mathbf{R}_5) \delta_{m,m-1} \delta_{n,n+1} + e^{i\theta_{m,n}^{m',n'}} E_{\mu\mu'}^{jj'}(\mathbf{R}_6) \delta_{m,m+1} \delta_{n,n+1}.
\end{aligned} \tag{2.16}$$

Now, for given flux ratio  $p/q$ , only the  $q$  determines the periodicity of the magnetic cell assuming  $p$  and  $q$  are mutually prime numbers. When we plot the band energies while varying the  $p$ , we obtain the famous Hofstadter butterfly<sup>3</sup>, a complex fractal structure as seen in Fig. 2.3. This structure is generated at the  $K = (\frac{4\pi}{3a}, 0)$  k-point. This fractal spectrum is a result of two competing effects, lattice periodicity and magnetic unit cell periodicity enforced by the presence of the magnetic field. Eq. 2.16 give the following matrix which must be diagonalized to obtain the energy eigenvalues.

The magnetic field enters the TB Hamiltonian only through the fraction  $p/q$ , which is the magnetic flux through the primitive unit cell of the lattice. In general, as the lattice geometry evolves, the area of the primitive unit cell changes  $(m + 1/2)$  times

An alternative approach to the derivation of the Hamiltonian under an uniform magnetic field is given in Appendix B.

## 2.3 Spin-orbit coupling

Due to the heavy mass of the transition-metal  $M$  atom, its spin orbit coupling(SOC) can be large. For the sake of simplicity, only the on-site contribution, namely, the  $\mathbf{L} \cdot \mathbf{S}$  term from  $M$  atoms. Using the bases  $\left\{ |d_{z^2}, \uparrow\rangle, |d_{xy}, \uparrow\rangle, |d_{x^2-y^2}, \uparrow\rangle, |d_{z^2}, \downarrow\rangle, |d_{xy}, \downarrow\rangle, |d_{x^2-y^2}, \downarrow\rangle \right\}$ , we get the SOC contribution to the Hamiltonian as

$$H' = \lambda \mathbf{L} \cdot \mathbf{S} = \frac{\lambda}{2} \begin{pmatrix} L_z & 0 \\ 0 & -L_z \end{pmatrix}, \tag{2.17}$$

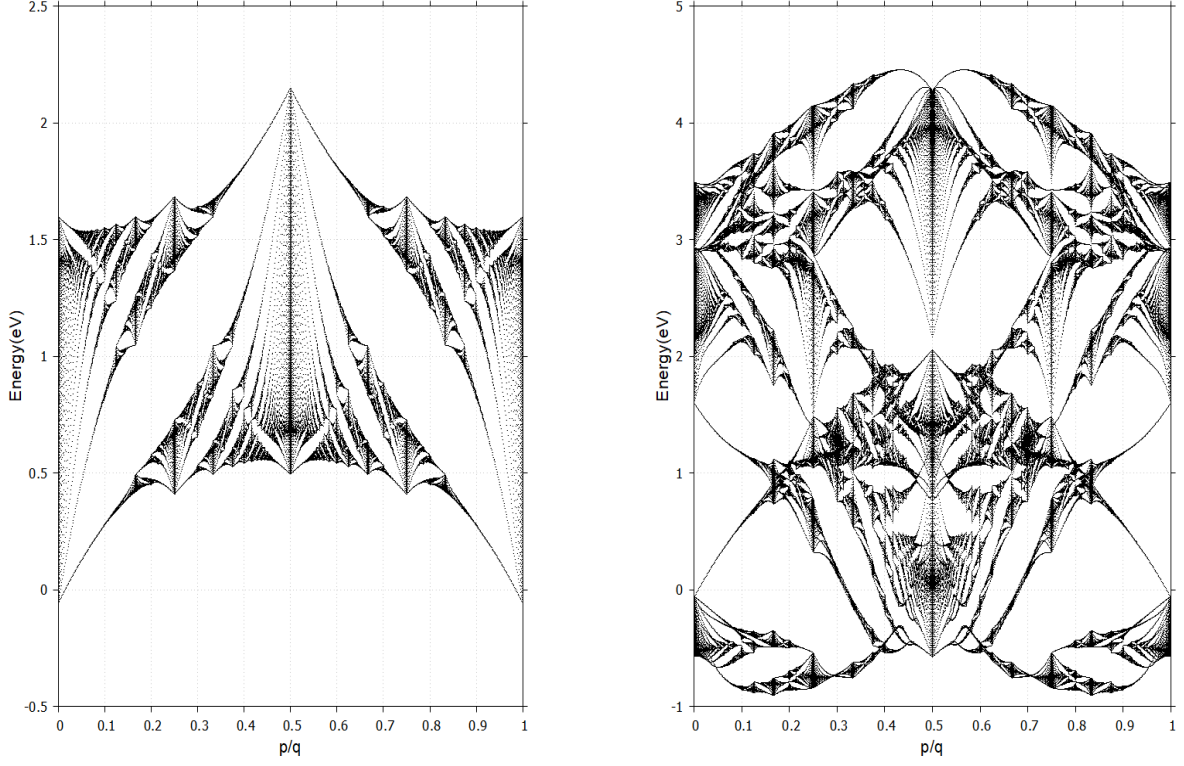


Figure 2.3: Hofstadter's butterfly for one band  $|dz\rangle \equiv |\phi_1^1(x, y)\rangle$  (left) and all band (right) with  $q = 797$  and vary  $p$  from 1 to  $q$  with field strength  $B_0 = 4.6928 \times 10^4$  T.

in which

$$L_z = \begin{pmatrix} 0 & 0 & 0 \\ 0 & 0 & 2i \\ 0 & -2i & 0 \end{pmatrix} \quad (2.18)$$

is the matrix of  $\hat{L}_z$  ( $z$  component of the orbital angular momentum) in bases of  $d_{z^2}$ ,  $d_{xy}$ ,  $d_{x^2-y^2}$  and  $\lambda$  is characterized the strength of the SOC. Noting that, under the three bases, the matrix elements of  $\hat{L}_x$  and  $\hat{L}_y$  are all zeros. There for the Hamiltonian for the magnetic unit cell with the SOC as follows

$$H_{\text{SOC}}(\mathbf{k})S = \mathbf{I}_2 \otimes H_0(\mathbf{k}) + H' \quad (2.19)$$

## 2.4 Landau levels

In solid-state physics, the behavior of electrons in magnetic fields is usually introduced by using the Hamiltonian

$$H = \frac{\mathbf{p} + e\mathbf{A}(\mathbf{r})^2}{2m}. \quad (2.20)$$

$$E = (n + 1/2) \hbar\omega_c \quad (2.21)$$

and the energy eigenfunctions are known as Landau levels.

This treatment is for free electrons,<sup>4</sup> but near the bottom of the two-dimensional tight-binding band of TMD, the energy is approximately free-electron-like by Taylor expanding to second order of  $\mathbf{k}$

$$\begin{aligned} E(\mathbf{k}) &\approx 2t_0 \left[ 1 - \frac{a^2 k_x^2}{2} + 2 \left( 1 - \frac{a^2 k_x^2}{8} \right) \left( 1 - \frac{3a^2 k_y^2}{8} \right) \right] \\ &= t_0 \frac{3}{16} (32 + a^4 k_x^2 k_y^2) - t_0 \frac{3}{2} a^2 (k_x^2 + k_y^2), \end{aligned} \quad (2.22)$$

the first term  $a^2$  is negligibly small and another can be treated like constant, then we have

$$E(\mathbf{k}) \approx 6t_0 - \frac{\hbar^2}{2m} (k_x^2 + k_y^2), \quad (2.23)$$

where  $m^* = \frac{\hbar^2}{(3t_0 a^2/4)}$  is the effective mass. Hence, the cyclotron frequency is

$$\omega_c = \frac{eB}{m^*} = \frac{\sqrt{3}}{2} t_0 \frac{p}{q}, \quad (2.24)$$

and therefore the Landau levels near the bottom of the band  $|d_{z^2}\rangle$  can be written as

$$E(\mathbf{k}) = t_0 \left( 6 - \sqrt{3} \frac{p}{q} (n + 1/2) \right), \quad (2.25)$$

in linear order of an uniform-flux, where  $n$  is Landau index.

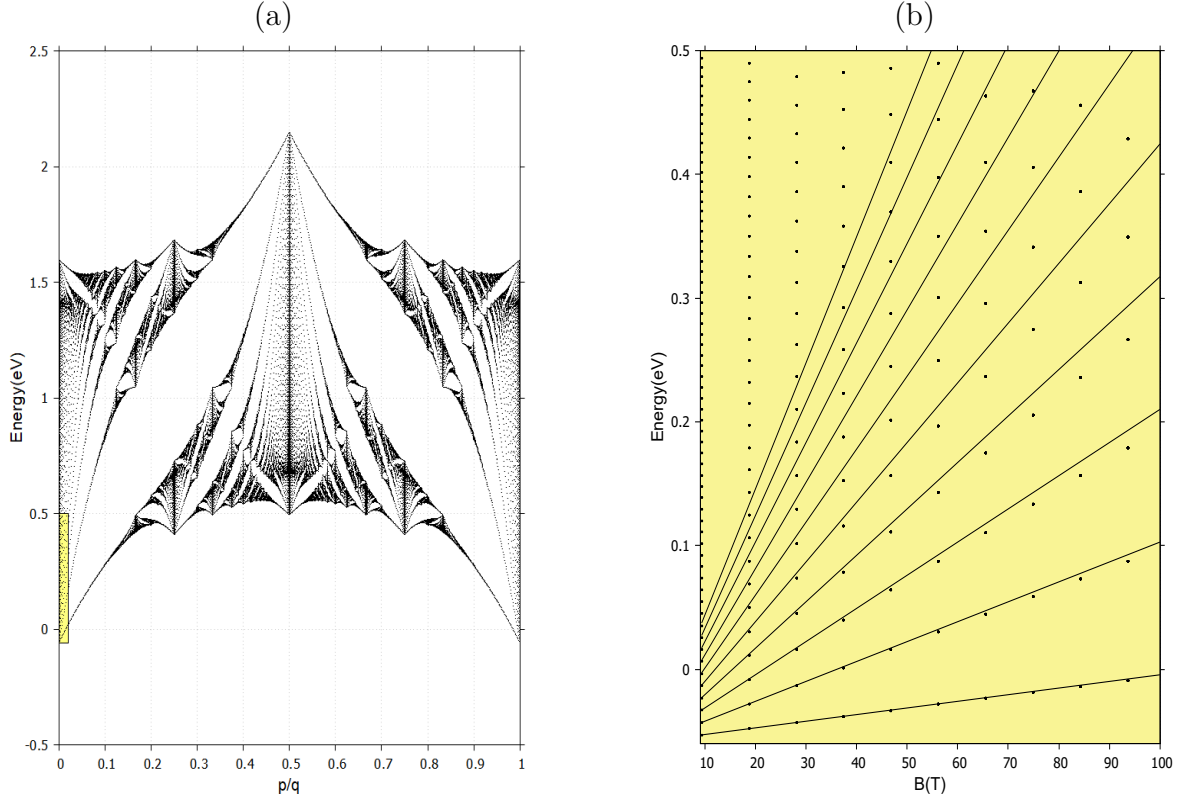


Figure 2.4: (a) Same plot as Fig 2.3 but we consider a small area and (b) is the Landau fan diagram show for the first  $n = 10$  levels near the bottom of the conduction band for a magnetic field up to  $B = 100$  T.

In Fig 2.4 we compare the spectrum of a small section of triangular lattice with  $p/q = 1/797$ . With the fan of Landau levels given by Eq.(2.26) plotted in Fig 2.4(b). The fan of Landau levels can be clearly seen emergin from the partern in Fig 2.4(a). It is this fan of Landau levels that responsiblee for the de Haas-van Alphen and Shubnikov-de Haas effects.<sup>5,6,7,8</sup> The Landau levels are all close to being linear in  $B$ , resulting from the magnetic quantization of parabolic bands at  $B = 0$ . In our model study, Landau levels can be classified into specific groups. In each group, each levels can be further labeled by a Landau index  $n$ . Figure 2.4 displays a blowup of the low uniform magnetic region and the LLs as a function of  $\Phi/\Phi_0$ <sup>9</sup>

## **CHAPTER 3**

### **DISCUSSION AND FUTURE WORK**

## REFERENCES

- [1] F. Yalçın, “Tight binding investigation of graphene nanostructures under magnetic field,” Master’s thesis, Middle East Technical University, 2019.
- [2] G.-B. Liu, W.-Y. Shan, Y. Yao, W. Yao, and D. Xiao, “Three-band tight-binding model for monolayers of group-vib transition metal dichalcogenides,” *Phys. Rev. B*, vol. 88, p. 085433, Aug 2013.
- [3] D. R. Hofstadter, “Energy levels and wave functions of bloch electrons in rational and irrational magnetic fields,” *Phys. Rev. B*, vol. 14, pp. 2239–2249, Sep 1976.
- [4] J. G. Analytis, S. J. Blundell, and A. Ardavan, “Landau levels, molecular orbitals, and the hofstadter butterfly in finite systems,” *American Journal of Physics*, vol. 72, pp. 613–618, 05 2004.
- [5] D. Shoenberg, *Magnetic Oscillations in Metals*. Cambridge Monographs on Physics, Cambridge University Press, 1984.
- [6] J. Singleton, *Band Theory and Electronic Properties of Solids*. Oxford Master Series in Condensed Matter Physics, OUP Oxford, 2001.
- [7] S. Blundell, *Magnetism in Condensed Matter*. Oxford Master Series in Condensed Matter Physics 4, OUP Oxford, 2001.
- [8] C. Kittel, *Quantum Theory of Solids*. Wiley, 1987.
- [9] J. Li, Y.-F. Wang, and C.-D. Gong, “Tight-binding electrons on triangular and kagomé lattices under staggered modulated magnetic fields: quantum hall ef-

- fects and hofstadter butterflies,” *Journal of Physics: Condensed Matter*, vol. 23, p. 156002, apr 2011.
- [10] A. Kormányos, V. Zólyomi, N. D. Drummond, P. Rakytá, G. Burkard, and V. I. Fal’ko, “Monolayer  $\text{mos}_2$ : Trigonal warping, the  $\Gamma$  valley, and spin-orbit coupling effects,” *Phys. Rev. B*, vol. 88, p. 045416, Jul 2013.
  - [11] F. Xuan and S. Y. Quek, “Valley zeeman effect and landau levels in two-dimensional transition metal dichalcogenides,” *Phys. Rev. Res.*, vol. 2, p. 033256, Aug 2020.
  - [12] J. J. Sakurai and J. Napolitano, *Modern quantum mechanics*. Cambridge University Press, 2020.
  - [13] P. G. Harper, “The general motion of conduction electrons in a uniform magnetic field, with application to the diamagnetism of metals,” *Proceedings of the Physical Society. Section A*, vol. 68, no. 10, pp. 879–892, 1955.
  - [14] Y. Aharonov and D. Bohm, “Significance of electromagnetic potentials in the quantum theory,” *Physical review*, vol. 115, no. 3, pp. 485–497, 1959.
  - [15] R. Peierls, “Zur theorie des diamagnetismus von leitungselektronen,” *Zeitschrift für Physik*, vol. 80, no. 11, pp. 763–791, 1933.
  - [16] G.-Y. Oh, “Energy spectrum of a triangular lattice in a uniform magnetic field: Effect of next-nearest-neighbor hopping,” *Journal of the Korean Physical Society*, vol. 37, no. 5, pp. 534–539, 2000.



## APPENDIX A

### Construct matrix

In Ref.<sup>2</sup>, G-B Liu *et al.* constructed

## APPENDIX B

### Harper's equation

Let us consider the case of hexagonal lattice with  $|d_{z^2}\rangle$  band as a basis under an uniform magnetic field given by the Landau gauge  $\vec{A} = (0, Bx, 0)$ . Given

$$\begin{aligned}
 h_0 &= 2t_0 (\cos 2\alpha + 2 \cos \alpha \cos \beta) + \epsilon_1 \\
 &= 2t_0 \left[ \cos(k_x a) + 2 \cos\left(\frac{k_x a}{2}\right) \cos\left(\frac{\sqrt{3}k_y a}{2}\right) \right] + \epsilon_1 \\
 &= 2t_0 \left\{ \cos(k_x a) + \cos\left[\left(k_x + \sqrt{3}k_y\right) \frac{a}{2}\right] + \cos\left[\left(k_x - \sqrt{3}k_y\right) \frac{a}{2}\right] \right\} + \epsilon_1 \\
 &= 2t_0 \left\{ \cos\left(p_x \frac{a}{\hbar}\right) + \cos\left[\left(p_x + \sqrt{3}eBx + \sqrt{3}p_y\right) \frac{a}{2\hbar}\right] \right. \\
 &\quad \left. + \cos\left[\left(p_x - \sqrt{3}eBx - \sqrt{3}p_y\right) \frac{a}{2\hbar}\right] \right\} + \epsilon_1 \tag{B.1} \\
 &= t_0 \left[ e^{ip_x \frac{a}{\hbar}} + e^{-ip_x \frac{a}{\hbar}} + e^{i(p_x + \sqrt{3}eBx + \sqrt{3}p_y)a/2\hbar} + e^{-i(p_x + \sqrt{3}eBx + \sqrt{3}p_y)a/2\hbar} \right. \\
 &\quad \left. + e^{i(p_x - \sqrt{3}eBx - \sqrt{3}p_y)a/2\hbar} + e^{-i(p_x - \sqrt{3}eBx - \sqrt{3}p_y)a/2\hbar} \right] + \epsilon_1.
 \end{aligned}$$

We replaced  $\hbar k$  in the above function by the operators  $\vec{p} - e\vec{A}/c$  in order to create an operator out of  $h_0$ . When this substitution is made, the Hamiltonian element is seen to contain translation operators  $\exp[ap_x/\hbar]$ ,  $\exp[a\sqrt{3}p_y/(2\hbar)]$ . Depending on the gauge chosen, there are, in addition, certain phase factors dependent on the magnetic field strength, which multiply the translation operators. The Landau gauge was  $\vec{A} =$

$(0, Bx, 0)$  was chosen, then only the translation along  $y$  are multiplied by phases.<sup>3</sup> Applying the BCH's formula and taking to account the commutation relation  $[x, p_x] = i\hbar$

$$\begin{aligned} e^{\pm i(p_x + \sqrt{3}eBx)a/2\hbar} &= e^{\pm ip_x a/2\hbar} e^{\pm i\sqrt{3}eBxa/2\hbar} e^{-\frac{1}{2}[\pm ip_x, \pm i\sqrt{3}eBx]a^2/2\hbar^2} \\ &= e^{\pm ip_x a/2\hbar} e^{\pm i\sqrt{3}eBxa/2\hbar} e^{\mp i\sqrt{3}eBa^2/8\hbar} \end{aligned} \quad (\text{B.2})$$

Substituting  $x = \frac{ma}{2}$  into (B.2), this leads to

$$e^{\pm i(p_x + \sqrt{3}eBx)a/2\hbar} = e^{\pm ip_x a/2\hbar} e^{\pm i\sqrt{3}eB(m+1/2)a/4\hbar} \quad (\text{B.3})$$

And

$$\begin{aligned} e^{\pm i(p_x - \sqrt{3}eBx)a/2\hbar} &= e^{\pm ip_x a/2\hbar} e^{\mp i\sqrt{3}eBxa/2\hbar} e^{-\frac{1}{2}[\pm ip_x, \mp i\sqrt{3}eBx]a^2/2\hbar^2} \\ &= e^{\pm ip_x a/2\hbar} e^{\mp i\sqrt{3}eBxa/2\hbar} e^{\mp i\sqrt{3}eBa^2/8\hbar} \end{aligned} \quad (\text{B.4})$$

Substituting  $x = \frac{ma}{2}$  into (B.4), this leads to

$$e^{\pm i(p_x - \sqrt{3}eBx)a/2\hbar} = e^{\pm ip_x a/2\hbar} e^{\mp i\sqrt{3}eB(m-1/2)a^2/4\hbar} \quad (\text{B.5})$$

The operators  $e^{\pm ip_x a/2\hbar}$ ,  $e^{\pm ip_y \sqrt{3}a/2\hbar}$  can be regconized as translational operators, we can rewrite (B.1) as The time-indepentdent Schrödinger's equation now becomes

$$\begin{aligned} &t_0\varphi_1(x+a, y) + t_0\varphi_1(x-a, y) + t_0\varphi_1(x + \frac{a}{2}, y + \frac{a\sqrt{3}}{2})e^{\frac{ie}{\hbar}B(m+1/2)\frac{a^2\sqrt{3}}{4}} \\ &+ t_0\varphi_1(x + \frac{a}{2}, y - \frac{a\sqrt{3}}{2})e^{-\frac{ie}{\hbar}B(m+1/2)\frac{a^2\sqrt{3}}{4}} + t_0\varphi_1(x - \frac{a}{2}, y + \frac{a\sqrt{3}}{2})e^{\frac{ie}{\hbar}B(m+1/2)\frac{a^2\sqrt{3}}{4}} \\ &+ t_0\varphi_1(x - \frac{a}{2}, y - \frac{a\sqrt{3}}{2})e^{-\frac{ie}{\hbar}B(m-1/2)\frac{a^2\sqrt{3}}{4}} + \epsilon_1\varphi_1(x, y) = E_1\varphi_0(x, y), \end{aligned} \quad (\text{B.6})$$

for the sake of simplicity let us define  $\varphi_0 \equiv |d_{z^2}\rangle$ .

It is reasonable to assume planewave behavior in the  $y$  direction, since the coefficents in the above equation only involve  $x$ . Therefore, we can assume the partial solution for  $y$

to be in the form

$$\varphi\left(\frac{ma}{2}, \frac{na\sqrt{3}}{2}\right) = e^{ik_y n \frac{a\sqrt{3}}{2}} G(m), \quad (\text{B.7})$$

which reduces (B.6) to

$$\begin{aligned} & t_0\varphi_0(m+2) + t_0\varphi_0(m-2) + t_0\varphi_0(m+1)e^{2i\pi(m+1/2)p/q}e^{ik_y a\sqrt{3}/2} \\ & + t_0\varphi_0(m+1)e^{-2i\pi(m+1/2)p/q}e^{-ik_y a\sqrt{3}/2} + t_0\varphi_0(m-1)e^{2i\pi(m-1/2)p/q}e^{ik_y a\sqrt{3}/2} \\ & + t_0\varphi_0(m-1)e^{-2i\pi(m-1/2)p/q}e^{-ik_y a\sqrt{3}/2} + \epsilon_1\varphi_0(m) = E_1\varphi_0(m), \end{aligned} \quad (\text{B.8})$$

this is equivalent to Eq. 2.16 we have mentioned in Section 2.2. Equation B.7 is sometimes called “Harper’s equation”.<sup>13</sup> Since different  $m$  values give different equations, one reaches a unique set of equations when  $\Phi/\Phi_0$  is a rational number  $p/q$  and  $m$  goes through  $q$  different values, essentially resulting in the Hamiltonian matrix written for a magnetic unit cell enlarged in  $x$  direction  $q$  times.

## APPENDIX C

### Phase factor

$$\begin{aligned}
H_{\mu\mu'}^{jj'}(\mathbf{k}) &= \sum_{\mathbf{R}} e^{\frac{ie}{\hbar} \int_0^{\mathbf{R}} A(\mathbf{r}') \cdot d\mathbf{r}'} e^{i\mathbf{k} \cdot \mathbf{R}} E_{\mu\mu'}^{jj'}(\mathbf{R}) \\
&= E_{\mu\mu'}^{jj'}(\mathbf{0}) + e^{\frac{ie}{\hbar} \int_0^{\mathbf{R}_1} \mathbf{A}(\mathbf{r}') \cdot d\mathbf{r}'} e^{i\mathbf{k} \cdot \mathbf{R}_1} E_{\mu\mu'}^{jj'}(\mathbf{R}_1) \\
&\quad + e^{\frac{ie}{\hbar} \int_0^{\mathbf{R}_2} \mathbf{A}(\mathbf{r}') \cdot d\mathbf{r}'} e^{i\mathbf{k} \cdot \mathbf{R}_2} E_{\mu\mu'}^{jj'}(\mathbf{R}_2) + e^{\frac{ie}{\hbar} \int_0^{\mathbf{R}_3} \mathbf{A}(\mathbf{r}') \cdot d\mathbf{r}'} e^{i\mathbf{k} \cdot \mathbf{R}_3} E_{\mu\mu'}^{jj'}(\mathbf{R}_3) \\
&\quad + e^{\frac{ie}{\hbar} \int_0^{\mathbf{R}_4} \mathbf{A}(\mathbf{r}') \cdot d\mathbf{r}'} e^{i\mathbf{k} \cdot \mathbf{R}_4} E_{\mu\mu'}^{jj'}(\mathbf{R}_4) + e^{\frac{ie}{\hbar} \int_0^{\mathbf{R}_5} \mathbf{A}(\mathbf{r}') \cdot d\mathbf{r}'} e^{i\mathbf{k} \cdot \mathbf{R}_5} E_{\mu\mu'}^{jj'}(\mathbf{R}_5) \\
&\quad + e^{\frac{ie}{\hbar} \int_0^{\mathbf{R}_6} \mathbf{A}(\mathbf{r}') \cdot d\mathbf{r}'} e^{i\mathbf{k} \cdot \mathbf{R}_6} E_{\mu\mu'}^{jj'}(\mathbf{R}_6) \\
&= E_{\mu\mu'}^{jj'}(\mathbf{0}) + e^{\frac{ie}{\hbar} Bx \int_0^{\mathbf{R}_1} dy} e^{ik_x a} E_{\mu\mu'}^{jj'}(\mathbf{R}_1) + e^{\frac{ie}{\hbar} Bx \int_0^{\mathbf{R}_2} dy} e^{ik_x \frac{a}{2}} e^{-ik_y \frac{a\sqrt{3}}{2}} E_{\mu\mu'}^{jj'}(\mathbf{R}_2) \\
&\quad + e^{\frac{ie}{\hbar} Bx \int_0^{\mathbf{R}_3} dy} e^{-ik_x \frac{a}{2}} e^{-ik_y \frac{a\sqrt{3}}{2}} E_{\mu\mu'}^{jj'}(\mathbf{R}_3) + e^{\frac{ie}{\hbar} Bx \int_0^{\mathbf{R}_4} dy} e^{-ik_x a} E_{\mu\mu'}^{jj'}(\mathbf{R}_4) \\
&\quad + e^{\frac{ie}{\hbar} Bx \int_0^{\mathbf{R}_5} dy} e^{-ik_x a} e^{ik_y \frac{a\sqrt{3}}{2}} E_{\mu\mu'}^{jj'}(\mathbf{R}_5) + e^{\frac{ie}{\hbar} Bx \int_0^{\mathbf{R}_6} dy} e^{ik_x a} e^{ik_y \frac{a\sqrt{3}}{2}} E_{\mu\mu'}^{jj'}(\mathbf{R}_6) \\
&= E_{\mu\mu'}^{jj'}(\mathbf{0}) + e^0 e^{ik_x a} E_{\mu\mu'}^{jj'}(\mathbf{R}_1) + e^{-\frac{ie}{\hbar} Bx \frac{a\sqrt{3}}{2}} e^{ik_x \frac{a}{2}} e^{-ik_y \frac{a\sqrt{3}}{2}} E_{\mu\mu'}^{jj'}(\mathbf{R}_2) \\
&\quad + e^{-\frac{ie}{\hbar} Bx \frac{a\sqrt{3}}{2}} e^{-ik_x \frac{a}{2}} e^{-ik_y \frac{a\sqrt{3}}{2}} E_{\mu\mu'}^{jj'}(\mathbf{R}_3) + e^0 e^{-ik_x a} E_{\mu\mu'}^{jj'}(\mathbf{R}_4) \\
&\quad + e^{\frac{ie}{\hbar} Bx \frac{a\sqrt{3}}{2}} e^{-ik_x a} e^{ik_y \frac{a\sqrt{3}}{2}} E_{\mu\mu'}^{jj'}(\mathbf{R}_5) + e^{\frac{ie}{\hbar} Bx \frac{a\sqrt{3}}{2}} e^{ik_x a} e^{ik_y \frac{a\sqrt{3}}{2}} E_{\mu\mu'}^{jj'}(\mathbf{R}_6)
\end{aligned} \tag{C.1}$$

Applying the BCH formula, and using the commutation relation  $[x, p_x] = i\hbar$ , we have

$$e^{i\left(\frac{\hbar k_x}{\hbar} - \frac{e}{\hbar} Bx\sqrt{3}\right)\frac{a}{2}} = e^{i(p_x - \sqrt{3}eBx)\frac{a}{2\hbar}} = \tag{C.2}$$